Inorganic Chemistry
Article

Inorg. Chem. **2009**, *48*, 5177–5186 **5177**
DOI: 10.1021/ic9001048

In Situ Ligand Transformation in the Synthesis of Manganese Complexes: Mono-, Tri- and a Barrel-shaped Tetradeca-nuclear Mn^{II}_{14} Aggregate

Muhammad Usman Anwar,[†] Yanhua Lan,[†] Lianne M. C. Beltran,[†] Rodolphe Clérac,[‡,§] Sven Pfirrmann,[†] Christopher E. Anson,[†] and Annie K. Powell*[,†]

[†]*Institut für Anorganische Chemie der Universität Karlsruhe, Engesserstrasse 15, 76131 Karlsruhe, Germany,* [‡]*CNRS, UPR 8641, Centre de Recherche Paul Pascal (CRPP), Equipe "Matériaux Moléculaires Magnétiques", 115 avenue du Dr. Albert Schweitzer, Pessac, F-33600, France, and* [§]*Université de Bordeaux, UPR 8641, Pessac, F-33600, France*

Received January 19, 2009

Three one-pot syntheses leading to four examples of in situ ligand transformations are presented. These in situ reactions involve various transformations of 2-(*N'*-dicyanomethylene-hydrazino)-benzoic acid (DHB). The resulting ligands enabled the preparation of three new coordination compounds, which were fully characterized by infrared spectroscopy, elemental analysis, and single crystal X-ray diffraction. The complex, $[Mn^{II}(Lig\text{-}I)(CH_3OH)Cl]$ (**1**), was prepared in a one-pot synthesis in which the aryl hydrazone ligand, $(Lig\text{-}I)^{2-}$, was formed by the amination of DHB resulting from the nucleophilic attack of an amino group of ethylenediamine. The linear, mixed-valence trinuclear complex, $(Et_3NH)_4[Mn^{III}_2Mn^{II}(\mu\text{-}OH)_2(Lig\text{-}II)_2(HLig\text{-}II)_2]$ (**2**), was synthesized using a preparation involving the in situ reaction of azide and a nitrile of DHB. Larger species can also be prepared using this technique. In a reaction involving two different in situ ligand formations, the cyclocondensation of two DHB molecules and the partial hydrolysis of a nitrile of DHB, the first example of a tetradecanuclear Mn(II) aggregate, $(H_3O)_4[Mn^{II}_{14}(\mu_6\text{-}CO_3)(\mu_3\text{-}OH)_6(HLig\text{-}III)_6(HLig\text{-}IV)_3(OH_2)_3]\cdot 92MeCN$ (**3**), was isolated and characterized. Magnetic measurements on **2** indicate the presence of intramolecular and intermolecular antiferromagnetic interactions ($J_1/k_B = -9.5(1)$ K, $g = 1.95(2)$, and $zJ'/k_B = -0.37(5)$ K) while those on **3** suggest the presence of dominating antiferromagnetic interactions.

Introduction

The synthesis of polynuclear transition metal compounds has long been an area of interest because of the presence of polymetallic groupings in biological[1] and molecule-based magnetic[2] systems. While these compounds are most often synthesized by the reaction of a metal precursor and a presynthesized ligand, it is also possible to generate the ligands in situ from an easily available organic compound. Since the report of a silver(I) system, the isolation of which involved the in situ synthesis of a tetrapyridyl ligand,[3] several other one-pot syntheses have been discovered and described.[4] This approach allows the reactivity of the metal ion to activate a proligand, transforming it through an in situ reaction, usually to give coordination compounds with ligands not normally accessible by conventional organic synthesis.

Aryl hydrazones are well-known for their coordination chemistry with different metals.[5] While organic chemists have extensively explored their nitrile derivatives to prepare heterocyclic compounds,[6] aryl hydrazones have not yet been investigated as ligand precursors in the synthesis of coordination compounds. In the presence of metal ions, additional electron-donating atoms can be incorporated by nucleophilic or electrophilic addition to the C≡N bond[7] forming new ligands. With this in mind, new coordination compounds were pursued using 2-(*N'*-dicyanomethylene-hydrazino)-benzoic acid (DHB) as a precursor. This aryl hydrazone already has two

*To whom correspondence should be addressed. E-mail: powell@aoc.uni-karlsruhe.de.

(1) (a) Lippard, S. J. *Angew. Chem., Int. Ed. Engl.* **1988**, *27*, 344. (b) Pope, M. T.; Müller, A. *Angew. Chem., Int. Ed. Engl.* **1991**, *30*, 34. (c) Katsoulis, D. E. *Chem. Rev.* **1998**, *98*, 359.

(2) (a) Gatteschi, D.; Sessoli, R. *Angew. Chem., Int. Ed.* **2003**, *42*, 268. (b) Boskovic, C.; Brechin, E. K.; Streib, W. E.; Folting, K.; Bollinger, J. C.; Hendrickson, D. N.; Christou, G. *J. Am. Chem. Soc.* **2002**, *124*, 3725–3736. (c) Sessoli, R.; Gatteschi, D.; Caneschi, A.; Novak, M. A. *Nature (London)* **1993**, *365*, 141.

(3) Blake, A. J.; Champness, N. R.; Chung, S. S. M.; Li, W.-S.; Schröder, M. *Chem. Commun.* **1997**, 1675.

(4) (a) Zhang, X.-M. *Coord. Chem. Rev.* **2005**, *249*, 1201–1219. (b) Zhao, H.; Qu, Z. R.; Ye, H. Y.; Xiong, R. G. *Chem. Soc. Rev.* **2008**, *37*, 84−100. (c) Evans, O. R.; Lin, W. *Acc. Chem. Res.* **2002**, *35*, 511–512. (d) Chen, X.-M.; Tong, M.-L. *Acc. Chem. Res.* **2007**, *40*, 162–170. (e) Cheng, L.; Zhang W.-X.; Ye, B.-H.; Lin, J.-B.; Chen, X. M. *Inorg. Chem.* **2007**, *46*, 1135–1143. (f) Feller, R. K.; Froster, P. M.; Wuddi, F.; Cheetham, A. K. *Inorg. Chem.* **2007**, *46*, 8717–8721. (g) Tong, M.-L.; Monfort, M.; Clemente, J. M.; Chen, X. -M.; Bu, X. H.; Ohba, M.; Kitagawa, S. *Chem. Commun.* **2005**, 233–235. (h) Zhang, C. -H.; Mao, H.-Y.; Wang, J.; Zhang, H.-Y.; Tao, J.-C. *Inorg. Chim. Acta* **2007**, *360*, 448–454.

Published on Web 05/11/2009

potentially coordinating functional groups, its carboxylic acid and its hydrazone. Transformations of its nitrile groups in the presence of manganese were expected to generate additional ligating sites, enabling the isolation of new manganese compounds. We report here three one-pot preparations involving in situ transformations of the nitriles of DHB (Figure 1) resulting in the syntheses of new manganese complexes of varying nuclearities: $[Mn^{III}(Lig\text{-}I)(CH_3OH)Cl]$ (**1**), $(Et_3NH)_4[Mn^{III}_2Mn^{II}(\mu\text{-}OH)_2(Lig\text{-}II)_2(HLig\text{-}II)_2]$ (**2**), and $(H_3O)_4[Mn^{II}_{14}(\mu_6\text{-}CO_3)(\mu_3\text{-}OH)_6(HLig\text{-}III)_6(HLig\text{-}IV)_3(OH_2)_3]\cdot 92MeCN$ (**3**).

Experimental Section

Material and Methods. The ligand 2-(*N*′-dicyanomethylene-hydrazino)-benzoic acid (DHB) was synthesized as previously reported.[8] Other reagents and solvents were used as received from commercial sources. The elemental analyses (CHN) were performed using an Elementar Vario EL analyzer. Fourier-transform IR spectra were measured on a Perkin-Elmer Spectrum One spectrometer with samples prepared as KBr disks.

X-ray Crystallography. Data were collected at 100 K on a Bruker SMART Apex CCD diffractometer with graphite-monochromated Mo-K_α radiation. Data were corrected for absorption using SADABS.[9] Structure solution by direct methods and full-matrix least-squares refinement against F^2 (all data) were carried out using SHELXTL.[10] All ordered non-H atoms were refined anisotropically. Organic H atoms were placed in calculated positions, while the coordinates of H atoms bonded to O or N were mostly refined with restrained N−H or O−H bond lengths. In the structure of **3**, both organic ligands were disordered. (HLig-III) is disordered about the crystallographic 2-fold axis running through C21, with concomitant disorder of the water ligand O14, which replaces the carboxylate oxygen O12. The nitrile group C30−N11 shows additional out-of-plane disorder. Each (HLig-IV) lies between two (HLig-III) ligands on the surface of the aggregate, and its position will therefore vary slightly depending on the orientations adopted by the two latter ligands. The resulting disorder could not be modeled satisfactorily, and the thermal ellipsoids of the ligand atoms are thus strongly elongated perpendicular to the plane of the ligand. The Mn_{14} aggregates are linked by H-bonding into a very open network, with the accessible solvent volume corresponding to 58.3% (31212 of 51850 Å^3) of the unit cell volume. It proved impossible to model the electron density within the cavity, and the four countercations (presumed to be H_3O^+ from the microanalytical data) and MeCN solvent molecules are not surprisingly badly disordered. The structure was therefore treated using the SQUEEZE option in the PLATON package,[11] and corrected for 2140 electrons per Mn_{14} formula unit, corresponding to the 4 $(H_3O)^+$ and 92 additional MeCN molecules.

Crystallographic data (excluding structure factors) for the structures in this paper have been deposited with the Cambridge Crystallographic Data Centre as supplementary publication nos. CCDC 713328−713330. Copies of the data can be obtained, free of charge, on application to CCDC, 12 Union Road, Cambridge CB2 1EZ, U.K.: http://www.ccdc.cam.ac.uk/perl/catreq/catreq.cgi, e-mail: data_request@ccdc.cam.ac.uk, or fax: +44 1223 336033.

Magnetic Measurements. The magnetic susceptibility measurements were obtained using a Quantum Design MPMS-XL SQUID magnetometer, functioning between 1.8 and 300 K for direct current (dc) applied fields ranging from −7 to 7 T. For alternating current (ac) susceptibility measurements, an oscillating ac field of 3 Oe and a frequency of 1000 Hz were employed, but a slow relaxation of magnetization was not observed in these compounds. For **2**, measurements were performed on 12.0 mg of dry, polycrystalline sample. Because of the uncertainty of the precise chemical formula of **3** when dry, a solid sample was measured in its mother liquor. Field-dependent magnetization measurements were performed at 100 K to ensure the absence of any ferromagnetic impurities. Corrections considering any diamagnetic contributions and the sample holder were applied to the raw magnetic data.

Synthesis of $[Mn^{III}(Lig\text{-}I)(CH_3OH)Cl]$ (1). A mixture of DHB (0.1 g, 0.46 mmol) and $MnCl_2\cdot 4H_2O$ (0.1 g, 0.5 mmol) was stirred together in 20 mL of MeOH. After 10 min, ethylenediamine (0.068 mL, 1.13 mmol) was added, and the solution color changed from yellow to dark brown. The mixture was stirred for 1 h to ensure completion of the reaction. Black crystals appeared after the solution was allowed to sit undisturbed for an hour. Yield: 60%. Selected IR data (KBr disk, cm^{-1}): 3350 (br), 2224 (m), 1651 (m), 1597 (s), 1577 (s), 1475 (w), 1435 (s), 1344 (m), 1272 (w), 1241 (w), 1147 (w), 1016 (m), 875 (w), 768 (m), 728 (w), 604 (w), 434 (w). Anal. Calcd (Found) for $C_{13}H_{16}N_6O_3MnCl$ (%): C, 39.56 (39.84); H, 4.09 (4.10); N, 21.29 (20.83).

Synthesis of $(Et_3NH)_4[Mn^{III}_2Mn^{II}(\mu\text{-}OH)_2(Lig\text{-}II)_2(HLig\text{-}II)_2]$ (2). DHB (0.1 g, 0.46 mmol), $MnCl_2\cdot 4H_2O$ (0.1 g, 0.5 mmol), and NaN_3 (0.06 g, 0.92 mmol) were stirred together in 20 mL of MeCN. After 10 min, triethylamine (0.13 mL, 0.9 mmol) was added. The reaction mixture was stirred for 2 h

(5) (a) Mishra, L.; Yadaw, A. K.; Srivastava, S.; Patel, A. B. *New J. Chem.* **2000**, *24*, 505. (b) Marten, J.; Seichter, W.; Weber, E. Z. *Anorg. Allg. Chem.* **2005**, *631*, 869–877. (c) Ghoneim, M. M.; El-Hallag, I. S.; El-Baradie, K. Y.; El-Desoky, H. S.; El-Attar, M. A. *Monatsh. Chem.* **2006**, *137*, 285–299. (d) Kelly, T. L.; Milway, V. A.; Grove, H.; Niel, V.; Abedin, T. S. M.; Thompson, L. K.; Zhao, L.; Harvey, R. G.; Miller, D. O.; Leech, M.; Goeta, A. E.; Howard, J. A. K. *Polyhedron* **2005**, *24*, 807–821. (e) EI-Bahnasawy, R. M.; EI-Meleigy, S. E. *Trans. Met. Chem.* **1994**, *19*, 270–274. (f) Crzybowski, J. J.; Allen, R. D.; Belinski, J. A.; Bieda, K. L.; Bish, T. A.; Fiegan, P. A.; Hartemstein, M. L.; Regitz, C. S.; Ryalls, D. M.; Quires, M. E.; Thoma, H. J. *Inorg. Chem.* **1993**, *32*, 5266–5272. (g) Ranford, J. H.; Vittal, J. J.; Wang, Y. M. *Inorg. Chem.* **1998**, *37*, 1226–1231. (h) Albertin, G.; Antoniutti, S.; Bacchi, A.; Marchi, F. D.; Pelizzi, G. *Inorg. Chem.* **2005**, *44*, 8947. (i) Bernhardt, P. V.; Mattsson, J.; Richardson, D. R. *Inorg. Chem.* **2006**, *45*, 752. (j) Gavrielatos, E.; Mitsos, C.; Athanasellis, G.; Heaton, B. T.; Steiner, A.; Bickley, J. F.; Markopoulou, O. I.; Markopoulos, J. *J. Chem. Soc., Dalton Trans.* **2001**, 639–644. (k) Gudasi, K. B.; Patil, S. A.; Vadavi, R. S.; Shenoy, R. V.; Nethaji, M.; Bligh, S. W. A. *Inorg. Chim. Acta* **2006**, *359*, 3229–3236.

(6) (a) Schäfer, H.; Gewald, K.; Gruner, M. *J. Prakt. Chem.* **1989**, *331*, 878–883. (b) Butler, R. N.; Quinn, K. F.; Welke, B. *J. Chem. Soc., Chem. Commun.* **1992**, 1481. (c) Shvekhgeimer, M.-G. A.; Ushakova, O. A. *Chem. Heterocycl. Compd.* **2001**, *37*, 370. (d) Tsai, P. C.; Wang, I. J. *Dyes Pigm.* **2005**, *64*, 259–264. (e) Kryštof, V.; Cankař, P.; Fryšová, I.; Slouka, J.; Kontopidis, G.; Džubák, P.; Hajdúch, M.; Srovnal, J.; de Azevedo, W. F.; Orság, X. M.; Paprskářová, M.; Rolčík, J.; Látr, A.; Fischer, P. M.; Strnad, M. *J. Med. Chem.* **2006**, *49*, 6500–6509. (f) Amer, A. M.; El-Bermaui, M. A.; Ahmed, A. F. S.; Soliman, S. M. *Monatsh. Chem.* **1999**, *130*, 1409–1418. (g) Amer, A. M. *Monatsh. Chem.* **2001**, *132*, 859–870. (h) Amer, A. M.; El-Mobayed, M. M.; Asker, S. *Monatsh. Chem.* **2004**, *135*, 595–604. (i) Schäfer, H.; Gewald, K.; Bellmann, P.; Gruner, M. *Monatsh. Chem.* **1991**, *122*, 195–207. (j) Fahmy, S. M.; Mohareb, R. N. *Tetrahedron* **1986**, *42*, 687.

(7) (a) Kukushkin, V. Y.; Pombeiro, A. J. L. *Chem. Rev.* **2002**, *102*, 1771–1802. (b) Chesman, A. S. R.; Turner, D. R.; Price, D. J.; Moubaraki, B.; Murray, K. S.; Deacon, G. B.; Batten, S. R. *Chem. Commun.* **2007**, 3541–3543. (c) Turner, D. R.; Pek, S. N.; Cashion, J. D.; Moubaraki, B.; Murray, K. S.; Batten, S. R. *Dalton Trans.* **2008**, 6877–6879. (d) Price, D. J.; Batten, S. R.; Berry, K. J.; Moubaraki, B.; Murray, K. S. *Polyhedron* **2003**, *22*, 165 – 176.

(8) Merlin, J. C. W.; Thomas, E. W.; Petit, G. *Can. J. Chem.* **1985**, *63*, 1840–1844.

(9) G. M. Sheldrick *SHELXTL 6.12*; Bruker AXS Inc.: Madison, WI, 2003.

(10) G. M. Sheldrick, *SADABS, the Siemens Area Detector Absorption Correction*; University of Göttingen: Göttingen, Germany, 2005.

(11) Spek, A. L. *J. Appl. Crystallogr.* **2003**, *36*, 7–13.

and then allowed to remain undisturbed for 3 days. Black cubic crystals were then obtained after filtration. Yield: 61%. Selected IR data (KBr disk, cm^{-1}): 3472 (br), 3193 (w), 2988 (w), 2701 (br), 2501 (s), 2218 (m), 1604 (s), 1589 (s), 1556 (s), 1490 (s), 1459 (s), 1487(s), 1422 (w), 1383 (s), 1356 (w), 1291 (w), 1217 (s), 1174 (s), 1032 (w), 882 (w), 776 (w), 748 (m), 602 (w), 552 (w), 424 (w). Anal. Calcd (Found) for $C_{64}H_{84}N_{32}O_{10}Mn_3$ (%): C, 47.25 (46.86); H, 5.21 (5.18); N, 27.57 (27.77).

Synthesis of $(H_3O)_4[Mn^{II}_{14}(\mu_6\text{-}CO_3)(\mu_3\text{-}OH)_6(HLig\text{-}III)_6(HLig\text{-}IV)_3(OH_2)_3]\cdot 92MeCN$ (3). An acetonitrile solution of DHB (0.1 g, 0.46 mmol), $MnCl_2\cdot 4H_2O$ (0.1 g, 0.5 mmol), and triethylamine (0.13 mL, 0.90 mmol) was refluxed for 30 min. It was then stirred at room temperature for 1 h, during which the color of the solution changed from yellow to dark red. The mixture was filtered and allowed to stand at room temperature. Dark red crystals appeared after 1 week. Yield 10%. Selected IR data (KBr disk, cm^{-1}): 3370 (br), 2219 (m), 1654 (w), 1586 (br, s), 1545 (s), 1510 (w), 1478 (br, s), 1388 (br, s), 1290 (m), 1247 (w), 1220 (w), 1158 (w), 973 (w), 857 (w), 761 (m), 492 (w). Anal. Calcd for $C_{159}H_{117}Mn_{14}N_{61}O_{58}$ (corresponding to loss of 88 of the 92 MeCN) (%): C, 41.71; H, 2.58; N, 18.66; found for samples of **3** dried in vacuo (%): C, 42.06; H, 2.72; N, 18.41.

Results and Discussion

Syntheses. The reaction of DHB with $MnCl_2\cdot 4H_2O$ and ethylenediamine in methanol afforded dark brown crystals of $[Mn^{III}(Lig\text{-}I)(CH_3OH)Cl]$ (**1**) in 60% yield. The synthesis involves an in situ ligand formation, in which DHB undergoes an amination by ethylenediamine resulting in the formation of $(Lig\text{-}I)^{2-}$; Figure 1 Scheme 1, shows its neutral form. One end of the base becomes bonded to the nitrilo carbon atom of the aryl hydrazone while the nitrilo nitrogen is converted into an amino group. Examples of in situ aminations are uncommon,[4] but this reaction is particularly interesting because two amines and two nitriles are present. Attempts to convert the second nitrile using excess base, excess manganese chloride, or longer reflux periods were unsuccessful. As for the second amine, no evidence of it reacting was observed, probably because the single amination results in a tetradentate ligand that can conveniently chelate a manganese center.

When DHB is combined with $MnCl_2\cdot 4H_2O$ and sodium azide in acetonitrile and triethylamine is used as the base, black crystals of the mixed-valent, trinuclear complex, $(Et_3NH)_4[Mn^{III}_2Mn^{II}(\mu\text{-}OH)_2(Lig\text{-}II)_2(H\text{-}Lig\text{-}II)_2]$ (**2**), were obtained in 61% yield. In this case, a [2 + 3] cycloaddition occurs between N_3^- and a nitrile of DHB forming a tetrazole *cis* to the amino group and resulting in anionic forms of $H_3Lig\text{-}II$ (Figure 1 Scheme 2). Attempts to react both nitrile groups were again unsuccessful. Previous examples of in situ tetrazole formation have mostly involved hydrothermal conditions;[4,12] so this preparation joins the few examples[10] where mild conditions are successful. Compound **2** is also the first linear, trinuclear manganese complex with a tetrazole-based ligand and is apparently very stable. Only a few manganese species have been reported to contain such ligands[12,13] despite the fact that their coordination chemistry has been subjected to much investigation.[14]

By heating a mixture of DHB, $MnCl_2\cdot 4H_2O$, and triethylamine in MeCN, a much larger species, $(H_3O)_4[Mn^{II}_{14}(\mu_6\text{-}CO_3)(\mu_3\text{-}OH)_6(HLig\text{-}III)_6(HLig\text{-}IV)_3(OH_2)_3]\cdot 92MeCN$ (**3**), can be obtained. In this reaction, two different in situ ligand formations originating from DHB take place. $(HLig\text{-}III)^{3-}$ results from a nitrile condensation involving two DHB molecules (Figure 1 Scheme 3). In the final ligand, two aryl hydrazonyl units have come together to form a heterocycle, as has been observed in a previously reported organic reaction.[6] The formation of the second ligand, $(HLig\text{-}IV)^{2-}$, involves the hydrolysis of the nitrile group *cis* to the amino group (Figure 1 Scheme 4). Additionally, some CO_3^{2-} was formed, presumably by the fixation of atmospheric CO_2. Its presence was confirmed by a strong band, $\nu_{CO3} = 1478\ cm^{-1}$ in the IR spectrum. These in situ formations enable the assembly of **3**, which is not only the first reported tetradecanuclear manganese-hydroxo compound, but also the largest Mn species isolated and characterized using the in situ ligand synthetic method.

Crystal Structure of 1. Dark brown crystals of **1** were analyzed using single-crystal X-ray diffraction (Table 1), and the complex was found to crystallize in the orthorhombic space group $P2_12_12_1$. The structure is shown in Figure 2, and selected interatomic distances and angles are listed in Table 2. The manganese ion is coordinated to a Cl^- ion, a methanol ligand, and the tetradentate $(Lig\text{-}I)^{2-}$, which has been deprotonated at its carboxyl oxygen and its hydrazonyl nitrogen (Figure 2a). In addition to the deprotonated atoms, $(Lig\text{-}I)^{2-}$ binds to the manganese center via imino and amino nitrogen atoms. The N5−C10 bond, which was formed during the in situ formation of $(Lig\text{-}I)^{2-}$, suggests double-bond character (1.313(3) Å). Short distances are also observed in the neighboring C10−N4 bond (1.342(3) Å) and the bonds of the hydrazone (N1−N2 1.307(3) Å; N2−C8 1.322(3) Å). This is unsurprising considering the number of possible resonance structures. As expected, the chelate bite angle of $(Lig\text{-}I)^{2-}$ formed by the five-membered ring (83.08(8)°) is smaller than that formed by the six-membered rings (93.09(7)° and 92.68 (8)°). Charge balance requires the manganese center to be trivalent, and this can also be confirmed from a bond valence sum (BVS) calculation[15] which gives a value of 3.18. As is typical of Mn(III), it has a tetragonally elongated octahedral geometry. Situated along its elongated Jahn−Teller axis are the O atom of the methanol ligand (Mn−O3 2.2702(19) Å) and the Cl^- ion (Mn−Cl 2.5915(7) Å). The packing of the molecules results in an alternating arrangement, where hydrogen bonding interactions are evident

(12) (a) Wang, L.-Z.; Qu, Z.-R.; Zhao, H.; Wang, X.-S.; Xiong, R.-G.; Xue, Z.-L. *Inorg. Chem.* **2003**, *42*, 3969. (b) Xiong, R.-G.; Xue, X.; Zhao, H.; You, X.-Z.; Abrahams, B. F.; Xue, Z. *Angew. Chem., Int. Ed.* **2002**, *41*, 3800. (c) Xue, X.; Wang, X.-S.; Wang, L.-Z.; Xiong, R.-G.; Abrahams, B. F.; You, X.-Z.; Xue, Z.-L.; Che, C.-M. *Inorg. Chem.* **2002**, *41*, 6544. (d) Qu, Z.-R.; Zhao, H.; Wang, X.-S.; Li, Y.-H.; Song, Y.-M.; Liu, Y.-J.; Ye, Q.; Xiong, R.-G.; Abrahams, B. F.; Xue, Z.-L.; You, X.-Z. *Inorg. Chem.* **2003**, *42*, 7710. (e) Gao, E.-Q.; Liu, N.; Cheng, A.-L.; Gao, S. *Chem. Commun.* **2007**, 2470.

(13) (a) Lin, P.; Clegg, W.; Harrington, R. W.; Henderson, R. A. *Dalton Trans.* **2005**, 2388. (b) Becker, T. M.; Krause-Bauer, J. K.; Homrighausen, C. L.; Orchin, M. *Polyhedron* **1999**, *18*, 2563.

(14) (a) Ye, Q.; Li, Y.-H.; Song, Y.-M.; Huang, X.-F.; Xiong, R.-G.; Xue, Z. *Inorg. Chem.* **2005**, *44*, 3618. (b) Ye, Q.; Song, Y. -M.; Wang, G. -X.; Chen, K.; Fu, D.-W.; Chan, P. W. H.; Zhu, J.-S.; Huang, S. D.; Xiong, R. -G. *J. Am. Chem. Soc.* **2006**, *128*, 6554. (c) Xue, X.; Abrahams, B. F.; Xiong, R. -G.; You, X. -Z. *Aust. J. Chem.* **2002**, *55*, 495.

(15) Liu, W.; Thorp, H. H. *Inorg. Chem.* **1993**, *32*, 4102–4105.

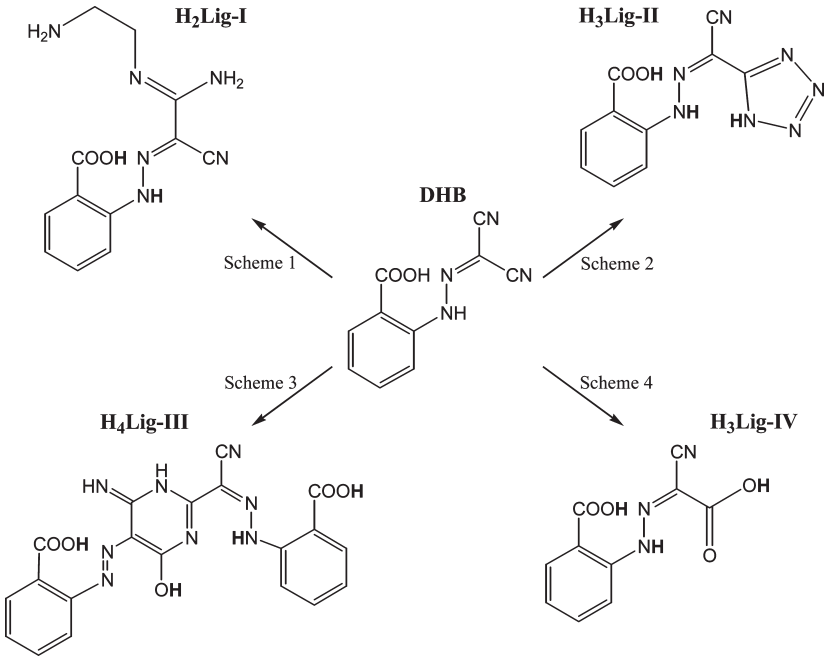

Figure 1. In situ formation of various ligands from DHB. Although ligands are shown in neutral form, all syntheses were carried out in basic media. Acidic protons are indicated in bold, but it should be noted that other resonance structures are possible for H_3LigII and H_4Lig-III.

Table 1. Crystallographic Data and Structure Refinement for Complexes **1**−**3**

	1	**2**	**3**
formula	$C_{13}H_{16}ClMnN_6O_3$	$C_{64}H_{84}Mn_3N_{32}O_{10}$	$C_{341}H_{387}Mn_{14}N_{150}O_{57}$
formula weight	394.71	1626.45	8268.17
crystal color	dark brown	black	dark red
crystal system	orthorhombic	monoclinic	trigonal
space group	$P2_12_12_1$	$P2_1/c$	$R\bar{3}c$
T [K]	100	100	100
a [Å]	6.9857(4)	11.3977(5)	33.681(2)
b [Å]	11.7814(7)	19.3147(9)	33.681(2)
c [Å]	18.9519(11)	17.6692(8)	52.778(3)
α [deg]	90	90	90
β [deg]	90	103.559(1)	90
γ [deg]	90	90	120
V [Å^3]	1559.77(11)	3781.3(3)	51850(6)
Z	4	2	6
d_c [g cm^{-3}]	1.618	1.428	1.589
F(000)	808	1694	25734
μ(Mo Kα) [mm^{-1}]	1.044	0.571	0.593
data measured	7872	17303	76533
unique data	3473	7394	11401
R_{int}	0.0188	0.0302	0.0845
parameters	233	571	407
wR_2 (all data)	0.0761	0.1454	0.1609
R_1 [$I \geq 2\sigma(I)$]	0.0294	0.0606	0.0611
S (all data)	1.050	1.065	0.963
largest diff. peak, hole	+0.43, −0.38	+0.53, −0.48	+0.70, −0.39
CCDC number	713328	713329	713330

between the chloride of each molecule and the methanolic, amino, and phenyl hydrogen atoms of neighboring molecules (2.3−2.8 Å, Figure 2b).

Crystal Structure of 2. Single-crystal X-ray diffraction revealed that the black crystals of **2** contain a trinuclear, anionic compound (Figure 3) and several triethylammonium ions. Experimental parameters are listed in Table 1 while bond distances and angles for the manganese centers can be found in Table 3. The compound crystallizes in the monoclinic space group, $P2_1/c$. In the trinuclear complex, a divalent manganese ion (Mn1) (the BVS calculation gives 1.96) residing on an inversion center is flanked by two trivalent manganese ions (Mn2 with BVS giving 3.18) with an interatomic Mn1···Mn2 distance of 3.3524(1) Å. Mn1 and Mn2 are linked together by a bridging hydroxyl group, a bridging carboxylate of a $(HLig\text{-}II)^{2-}$ ligand, and a bridging tetrazole of a $(Lig\text{-}II)^{3-}$ ligand. As can be seen in Scheme 2 in Figure 1, the neutral H_3Lig-II has an acidic proton in its acid, its hydrazone, and its tetrazole ring, respectively, all three of which are deprotonated in $(Lig\text{-}II)^{3-}$. With two N atoms of the tetrazole ring acting as donors, it has a total of four ligating sites. In addition to the tridentate chelation of Mn2 via the hydrazonyl nitrogen (N8), a carboxylate oxygen (O4), and a tetrazole nitrogen (N11), $(Lig\text{-}II)^{3-}$ bridges Mn1 and Mn2 through

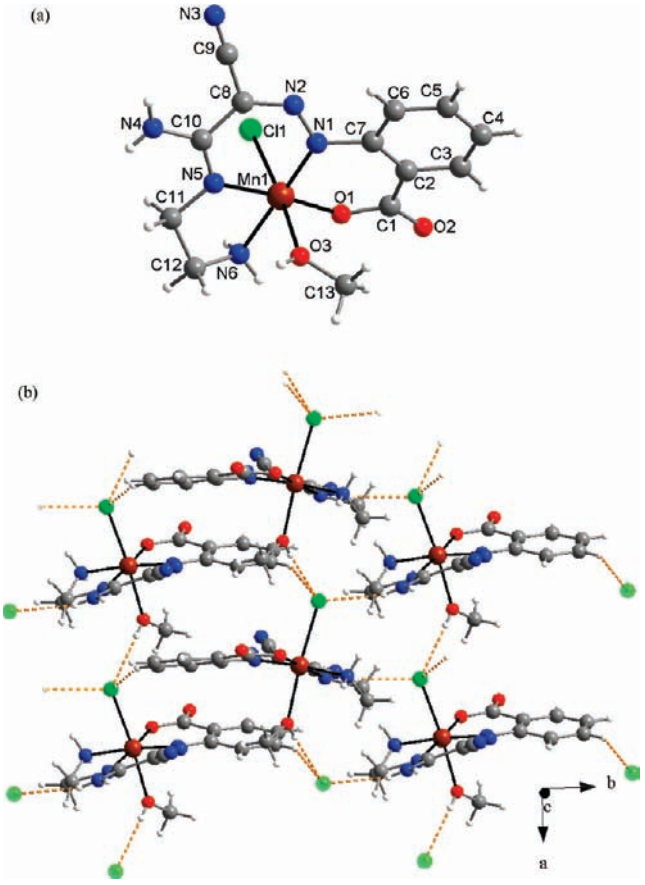

Figure 2. (a) Structure of $[Mn^{III}(Lig\text{-}I)(CH_3OH)Cl]$ in **1** and (b) a packing diagram where the intermolecular hydrogen bonds are shown as dashed orange lines. Color code: Mn, brown; Cl, green; O, red; N, blue; C, black; H, gray.

Table 2. Selected Bond Lengths (Å) and Angles (deg) for Complex **1**

Bond Lengths

Mn(1)−Cl(1)	2.5915(7)	N(2)−C(8)	1.322(3)
Mn(1)−O(1)	1.8747(16)	C(8)−C(9)	1.443(3)
Mn(1)−O(3)	2.2702(19)	C(8)−C(10)	1.464(3)
Mn(1)−N(1)	1.9601(19)	C(9)−N(3)	1.141(3)
Mn(1)−N(5)	1.9668(19)	C(10)−N(5)	1.313(3)
Mn(1)−N(6)	2.047(2)	C(10)−N(4)	1.342(3)
C(6)−C(7)	1.404(3)	N(5)−C(11)	1.480(3)
C(7)−N(1)	1.435(3)	C(11)−C(12)	1.519(3)
N(1)−N(2)	1.307(3)	C(12)−N(6)	1.480(3)

Bond Angles

C(1)−O(1)−Mn(1)	132.92(15)	N(1)−Mn(1)−O(3)	89.55(8)
O(1)−Mn(1)−Cl(1)	93.42(6)	N(1)−Mn(1)−N(5)	92.68(8)
O(1)−Mn(1)−O(3)	90.17(7)	N(1)−Mn(1)−N(6)	174.30(9)
O(1)−Mn(1)−N(1)	93.09(7)	N(5)−Mn(1)−Cl(1)	86.97(6)
O(1)−Mn(1)−N(5)	174.19(8)	N(5)−Mn(1)−O(3)	89.17(8)
O(1)−Mn(1)−N(6)	91.12(7)	N(5)−Mn(1)−N(6)	83.08(8)
O(3)−Mn(1)−Cl(1)	175.41(5)	N(6)−Mn(1)−Cl(1)	90.47(6)
N(1)−Mn(1)−Cl(1)	93.12(6)	N(6)−Mn(1)−O(3)	86.58(8)

a tetrazole (N11, N12). As for $(HLig\text{-}II)^{2-}$, the hydrazonyl nitrogen (N1) remains protonated and unbound, but its hydrogen has close contacts of approximately 2.2 Å to a tetrazole nitrogen (N4) and a carboxylate oxygen (O2). This ligand is tridentate and binds to all three metals through a *syn-syn* carboxylate bridge (O2, O3) and a tetrazole nitrogen (N5).

From the point of view of the metals, the octahedral coordination environment of Mn1 is composed of an oxygen

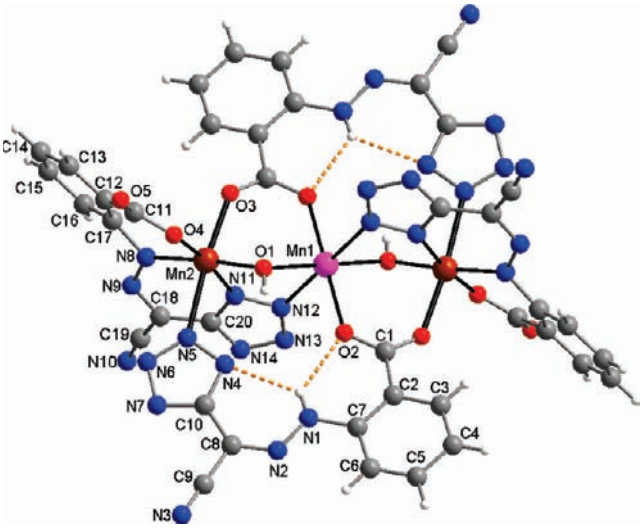

Figure 3. Structure of the trinuclear $[Mn_2^{III}Mn^{II}(\mu\text{-}OH)_2(Lig\text{-}II)_2(H\text{-}Lig\text{-}II)_2]^{4-}$ in **2**. For clarity, the Jahn−Teller axes of the trivalent Mn (Mn2) are indicated in bold, and the intramolecular hydrogen interactions are shown as dotted orange lines. Only one component of the modeled disorder in $(Lig\text{-}II)^{3-}$ is shown. Mn1 resides on a crystallographic inversion center. Color code: Mn(II), pink; Mn(III), brown; O, red; N, blue; C, black; H, gray.

Table 3. Selected Bond Distances (Å) and Angles (deg) for Complex **2**

Bond Lengths

Mn(1)−O(1)	2.115(2)	Mn(2)−O(4)	1.914(2)
Mn(1)−O(2)	2.242(2)	Mn(2)−N(5)	2.350(3)
Mn(1)−N(12)	2.276(3)	Mn(2)−N(8)	1.983(3)
Mn(2)−O(1)	1.895(2)	Mn(2)−N(11)	1.998(3)
Mn(2)−O(3)	2.117(2)	Mn(1)···Mn(2)	3.3524(1)

Bond Angles

Mn(1)−O(1)−Mn(2)	113.34(11)	O(1)−Mn(2)−N(11)	90.36(10)
O(1)−Mn(1)−O(1[a])	180.0(1)	O(3)−Mn(2)−N(5[a])	174.39(9)
O(1)−Mn(1)−N(12)	83.70(9)	O(4)−Mn(2)−O(3)	95.00(10)
O(1[a])−Mn(1)−O(2)	83.17(8)	O(4)−Mn(2)−N(5[a])	89.00(10)
O(2)−Mn(1)−O(2[a])	180.0	O(4)−Mn(2)−N(8)	90.52(12)
O(2)−Mn(1)−N(12)	90.63(9)	O(4)−Mn(2)−N(11)	171.83(11)
N(12)−Mn(1)−N(12[a])	180.0(1)	N(8)−Mn(2)−O(3)	92.76(10)
O(1)−Mn(2)−O(3)	90.74(9)	N(8)−Mn(2)−N(5[a])	91.13(10)
O(1)−Mn(2)−O(4)	91.58(10)	N(8)−Mn(2)−N(11)	87.05(12)
O(1)−Mn(2)−N(5[a])	85.21(10)	N(11)−Mn(2)−O(3)	92.91(10)
O(1)−Mn(2)−N(8)	175.75(11)	N(11)−Mn(2)−N(5[a])	83.26(10)

atom from the $(HLig\text{-}II)^{2-}$ carboxylate, a hydroxide, a nitrogen atom from the $(Lig\text{-}II)^{3-}$ tetrazole, and their symmetry equivalents. Being trivalent and high spin, Mn2 has a tetragonally elongated octahedral environment. A tetrazole nitrogen atom (N5) of a $(HLig\text{-}II)^{2-}$ ligand and a carboxylate oxygen atom (O3) of the symmetry-related $(HLig\text{-}II)^{2-}$ ligand coordinate along the Jahn−Teller axis. The bond lengths along this axis (Mn2−N5 2.350(3) Å; Mn2−O3 2.117(2) Å) are clearly longer than the equatorial bonds that Mn2 has with the bridging hydroxide and the $(Lig\text{-}II)^{3-}$ ligand. This arrangement of manganese centers is similar to that found by Murray et al. for two complexes which have ligands formed via an in situ reaction of dicyanonitrosomethanide with methanol or water solvent molecules.[7]

Crystal Structure of 3. Crystallographic analysis of **3** indicated a trigonal system in $R\bar{3}c$ (Table 1) containing a tetradecanuclear manganese-oxo aggregate surrounded by two different types of aryl hydrazone ligands, $[Mn_{14}^{II}(\mu_6\text{-}CO_3)(\mu_3\text{-}OH)_6(HLig\text{-}III)_6(HLig\text{-}IV)_3(OH_2)_3]^{4-}$

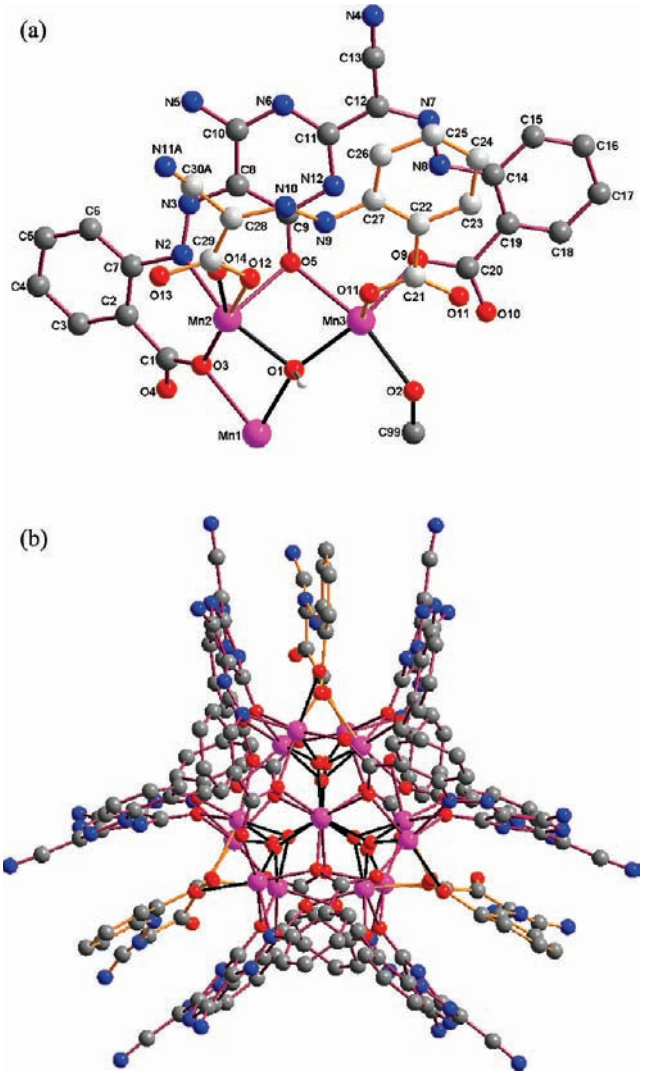

Figure 4. (a) Asymmetric unit of the aggregate in **3** and (b) the complete aggregate, $[Mn^{II}_{14}(\mu_6\text{-}CO_3)(\mu_3\text{-}OH)_6(HLig\text{-}III)_6(HLig\text{-}IV)_3(OH_2)_3]^{4-}$, viewed along its 3-fold axis. The center of the aggregate, C99, resides on a 32 symmetry site; Mn1 and O2 are located on 3-fold and 2-fold axes, respectively. For clarity, H atoms of the organic ligands have been omitted and only one component of the disordered $(HLig\text{-}IV)^{2-}$ is shown. $(H\text{-}Lig\text{-}III)^{3-}$ and $(HLig\text{-}IV)^{2-}$ are outlined in purple and orange, respectively. Color code for atoms: Mn, pink; C, gray; N, blue; O, red.

(Figure 4, Table 4). The fully protonated form of $(HLig\text{-}III)^{3-}$ is shown in Scheme 3 of Figure 1, but in **3** the hydroxyl and the acid groups of the ligand are deprotonated. The other ligand present, $(HLig\text{-}IV)^{2-}$, is the conjugate base of $H_3Lig\text{-}IV$ (Scheme 4 of Figure 1) in which the two carboxylic acids are deprotonated. In both $(HLig\text{-}III)^{3-}$ and $(HLig\text{-}IV)^{2-}$, the hydrazonyl amines remain protonated. Since the aggregate resides on a 32 symmetry site, its asymmetric unit (Figure 4a) represents only $^1/_6$th of the complete complex. At the center of the aggregate is a CO_3^{2-} in which each C99−O2 bond lies on a 2-fold rotational axis. All three independent manganese centers were clearly determined to be divalent based on the BVS calculations[15] with the values Mn1 2.08; Mn2 1.99; Mn3 1.97.

The 14 manganese ions are linked together from within by the carbonate (μ_6) and six hydroxide (μ_3) ligands. The resulting $Mn_{14}(CO_3)(OH)_6$ core is best described by

Table 4. Selected Bond Lengths (Å) and Angles (deg) for Complex **3**

Bond Lengths

Mn(1)···Mn(2)	3.1544(6)	Mn(2)−O(4[a])	2.201(3)
Mn(1)−O(1)	2.089(2)	Mn(2)−N(2)	2.228(3)
Mn(1)−O(3)	2.241(2)	Mn(3)−O(1)	2.139(2)
Mn(2)−O(1)	2.086(2)	Mn(3)−O(9)	2.143(2)
Mn(2)−O(3)	2.150(2)	Mn(3)−O(10[a])	2.155(2)
Mn(2)−O(12)	2.190(4)	Mn(3)−O(11)	2.197(2)
Mn(2)−O(14)	2.192(9)	Mn(3)−O(2)	2.2000(15)
Mn(2)−O(5)	2.201(2)	Mn(3)−O(5)	2.243(2)

Bond Angles

O(1)−Mn(1)−O(1)	102.37(8)	O(3)−Mn(2)−N(2)	79.97(10)
O(1[a])−Mn(1)−O(3)	167.30(9)	O(12)−Mn(2)−N(2)	104.81(15)
O(1[b])−Mn(1)−O(3)	89.29(8)	O(14)−Mn(2)−N(2)	89.7(2)
O(1)−Mn(1)−O(3)	79.68(8)	O(5)−Mn(2)−N(2)	75.28(11)
O(3[a])−Mn(1)−O(3)	87.84(9)	O(4[a])−Mn(2)−N(2)	109.52(11)
O(1)−Mn(2)−O(3)	81.88(9)	O(1)−Mn(3)−O(9)	169.98(9)
O(1)−Mn(2)−O(12)	96.90(14)	O(1)−Mn(3)−O(10[c])	91.06(8)
O(3)−Mn(2)−O(12)	172.81(14)	O(9)−Mn(3)−O(10[c])	88.94(9)
O(1)−Mn(2)−O(14)	117.8(2)	O(1)−Mn(3)−O(11)	88.27(9)
O(3)−Mn(2)−O(14)	156.0(2)	O(9)−Mn(3)−O(11)	89.04(9)
O(1)−Mn(2)−O(5)	78.78(8)	O(10[c])−Mn(3)−O(11)	164.38(9)
O(3)−Mn(2)−O(5)	106.19(9)	O(1)−Mn(3)−O(2)	87.64(6)
O(12)−Mn(2)−O(5)	80.43(14)	O(9)−Mn(3)−O(2)	102.13(7)
O(14)−Mn(2)−O(5)	91.9(2)	O(10[c])−Mn(3)−O(2)	102.79(8)
O(1)−Mn(2)−O(4[a])	101.15(9)	O(11)−Mn(3)−O(2)	92.77(8)
O(3)−Mn(2)−O(4[a])	84.96(9)	O(1)−Mn(3)−O(5)	76.76(8)
O(12)−Mn(2)−O(4[a])	88.33(14)	O(9)−Mn(3)−O(5)	93.34(9)
O(14)−Mn(2)−O(4[a])	78.1(2)	O(10[c])−Mn(3)−O(5)	81.45(9)
O(5)−Mn(2)−O(4[a])	168.64(9)	O(11)−Mn(3)−O(5)	83.20(9)
O(1)−Mn(2)−N(2)	142.55(11)	O(2)−Mn(3)−O(5)	163.97(7)
Mn(1)−O(1)−Mn(2)	98.15(9)	Mn(3)−O(2)−Mn(3[d])	114.39(12)
Mn(1)−O(1)−Mn(3)	128.61(11)	Mn(1)−O(3)−Mn(2)	91.83(8)
Mn(2)−O(1)−Mn(3)	105.75(9)	Mn(2)−O(5)−Mn(3)	98.59(8)

dividing it into three subunits, two outer identical tetranuclear units and a central hexanuclear unit (Figure 5). In the central unit, the CO_3^{2-} (C99, O2) connects the six Mn3 ions to give a trigonal antiprismatic (i.e., distorted octahedral) arrangement. The Mn3 ions can be divided into three pairs, each of which has two manganese ions joined by a carbonate oxygen (O2) and a *syn-syn* carboxylate (O11) of $(HLig\text{-}IV)^{2-}$. Mn3 centers originating from different pairs are linked by an additional *syn-syn* carboxylate (O9, O10) from $(HLig\text{-}III)^{3-}$. The octahedral coordination sphere of Mn3 is completed by linkages to the outer units of the complex; the phenoxy oxygen (O5) of $(HLig\text{-}III)^{3-}$ links Mn3 to Mn2 while a μ_3-OH bridge (O1) connects Mn3 to both Mn2 and Mn1.

The outer units of the aggregate are defined by three Mn2 ions surrounding a central Mn1 with Mn1···Mn2 distances of 3.1544(2) Å. As mentioned previously, it is held together by μ_3-OH bridges (O1) linking the outer subunits to Mn3 ions of the central unit. Mn2 and Mn1 are additionally linked by a *syn-syn* carboxylate bridge (O3, O4) of a $(HLig\text{-}III)^{3-}$ ligand and by a μ_2-O (O3) originating from the carboxylate of another $(HLig\text{-}III)^{3-}$. The latter ligand also chelates Mn2 by ligating at one of its hydrazonyl nitrogens (N2) and its phenoxy oxygen (O5). Overall, each $(HLig\text{-}III)^{3-}$ connects one Mn1 and two Mn2 centers via a *syn-syn-anti* carboxylate (O3, O4). Both Mn1 and Mn2 have octahedral coordination environments. The sixth site of Mn2 has been modeled for disorder; it is occupied by an oxygen atom that is part of a carboxylate group (O12) of $(HLig\text{-}IV)^{2-}$ or a terminal water ligand (O14). As shown in Figure 6, $(HLig\text{-}IV)^{2-}$ can be oriented in two different ways, connecting the central

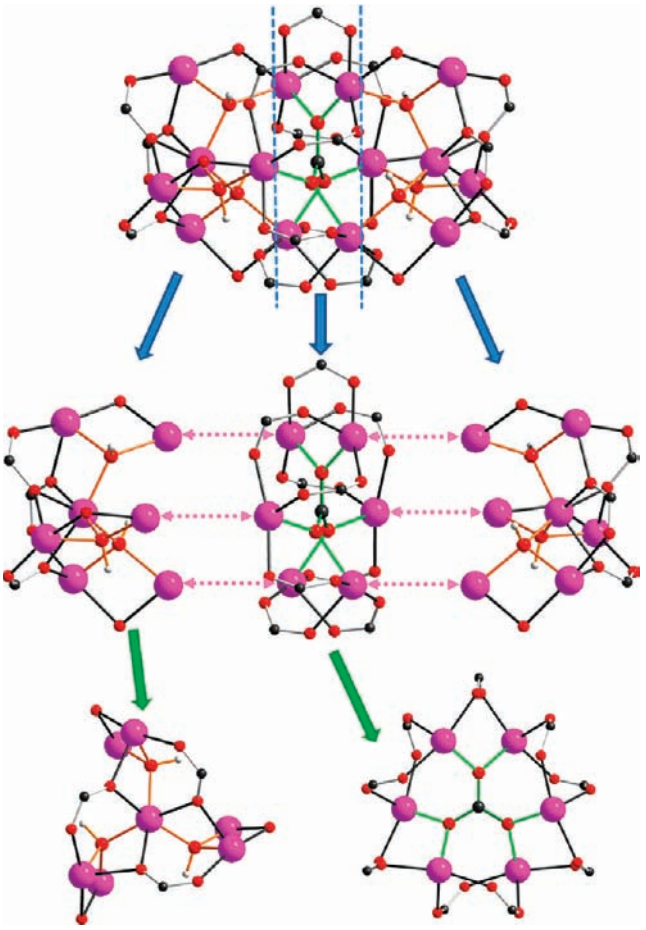

Figure 5. Inner $Mn_{14}(OH)_6(CO_3)$ core of **3** held together by carboxylate groups (top), how it can be broken down into central and outer portions (middle), and views of the fragments down the 3-fold axis (bottom). Dashed pink arrows indicate identical Mn centers while hydroxide and carbonate bonds have been highlighted in orange and green, respectively. Color code for atoms: Mn, pink; C, gray; O, red.

subunit to either of the outer subunits. The two orientations are related by the 2-fold rotational axes which coincide with the carbonato C−O bonds.

As observed in the $(HLig\text{-}II)^{2-}$ ligands of **2**, intramolecular hydrogen bonding is evident between these hydrazonyl H atoms and carboxylato O and imino N atoms (1.9−2.0 Å) in both $(HLig\text{-}III)^{3-}$ and $(HLig\text{-}IV)^{2-}$ (see Figures 6 and 7). Intermolecular hydrogen bonds are also present between $(HLig\text{-}III)^{3-}$ of neighboring aggregates (Figure 7). Subsequently, each Mn_{14} unit is hydrogen bonded to six other aggregates. This leads to a very open three-dimensional hydrogen-bonded network with a void space corresponding to about 57.6% of the unit cell volume (see Figure 8). Because of the packing arrangement, cavities rather than channels exist within the network. Within these cavities, the electron density cannot be resolved; any cations and solvent molecules are highly disordered. When the reaction conditions are considered, either hydronium or triethylammonium ions may be present for charge balance with the tetraanionic aggregate. Elemental analysis indicates that hydronium is the more likely candidate. As a result, the SQUEEZE routine in PLATON was used to evaluate and correct for the remaining electron density in the crystal structure;[11] the calculated electron density

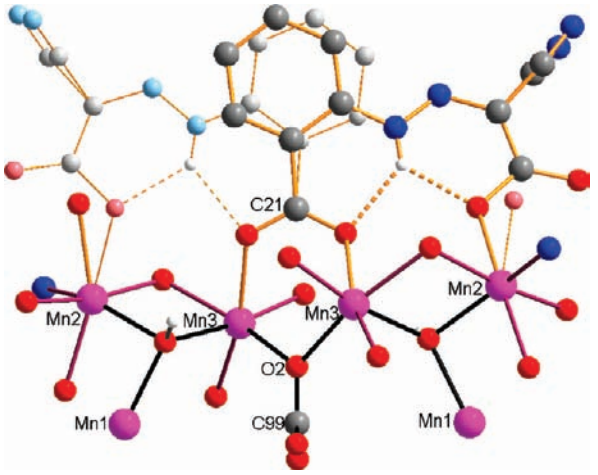

Figure 6. Modeled disorder of the $(HLig\text{-}IV)^{2-}$ and water ligands in **3**. The two components, differentiated by bond thickness and atom size, are related by a 2-fold axis that intersects with C99, O2, and C21. The H atoms of $(HLig\text{-}IV)^{2-}$ that do not take part in H bonding have been removed for clarity. Purple bonds are used to indicate bonds to $(HLig\text{-}III)^{3-}$. Color code for atoms: Mn, pink; C, gray; N, blue; O, red.

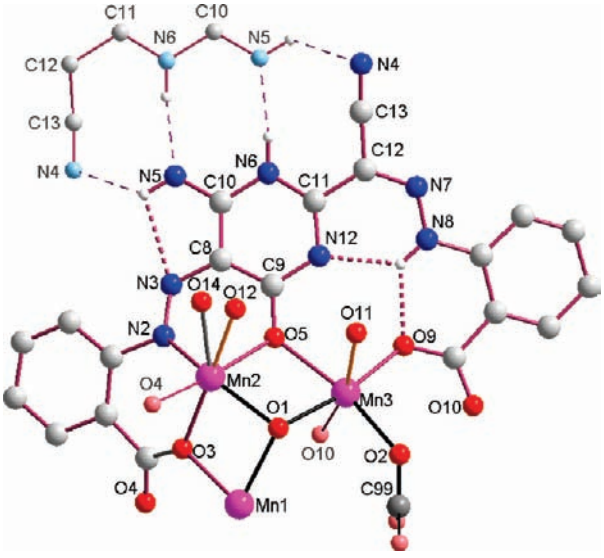

Figure 7. Manner in which $(HLig\text{-}III)^{3-}$ coordinates to the manganese ions and interacts with neighboring molecules in **3**. Purple bonds are used to indicate bonds of $(HLig\text{-}III)^{3-}$ while orange indicates those of $(HLig\text{-}IV)^{2-}$. Only H atoms involved in H bonding interactions are shown; intramolecular and intermolecular H interactions are represented by thick and thin dashed lines, respectively. Color code for atoms: Mn, pink; C, gray; N, blue; O, red.

corresponds to the four $(H_3O)^+$ cations and approximately 92 MeCN molecules. The single crystalline structure is not maintained when crystals are heated, suggesting that removal of MeCN molecules results in a collapse of this structure.

In comparison to the plethora of aggregates of Mn^{III} or mixed-valence Mn^{III}/Mn^{II}, far fewer oxygen-bridged aggregates only containing Mn^{II} have been reported. The largest is a Mn^{II}_{19} system with a planar core reported by Westin and co-workers,[16] while Mao et al. reported Mn^{II}_4 and Mn^{II}_6 compounds, which again have rather flat

(16) Du, Z.-Y.; Prosvirin, A. V.; Mao, J.-G. *Inorg. Chem.* **2007**, *46*, 9884–9894.

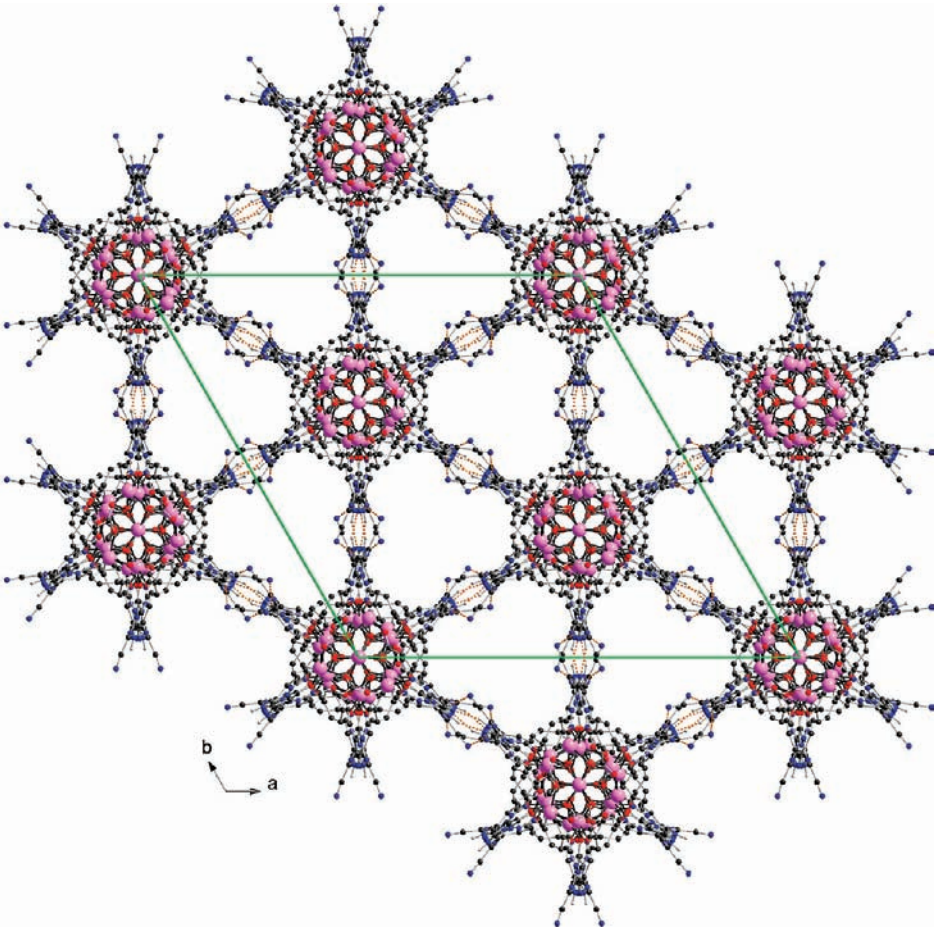

Figure 8. Packing of the aggregates viewed down the *c* axis. Color code for atoms: Mn, pink; C, gray; N, blue; O, red.

cores.[17] Compound **3** is thus the second-largest Mn^{II} aggregate so far reported, and the first such compound to have a core with a non-planar topology. A relevant example of an aggregate of fourteen $S = 5/2$ metal ions is furnished by the tetradecanuclear compound $[Fe_{14}(bta)_6O_6(OMe)_{18}Cl_6]$[18] where btaH is benzotriazole. This compound also has a non-planar core topology and a high spin ground state (see below). The main difference lies in the topology of the central six metals. If we notionally flatten out the central $\{\mu_6\text{-}(CO_3^{2-})Mn_6\}$ distorted octahedral core in **3** (Figure 5) to a planar hexagon, then a similar topology to that seen for Fe_{14} is realized.

Magnetic Properties of 2 and 3. The temperature-dependence of the magnetic susceptibility was measured for compounds **2** and **3** under an applied dc field of 1000 Oe. For compound **2**, the χT product is 8.0 cm^3 K mol^{-1} at room temperature (Figure 9). This value is quite low in comparison to the value expected for one Mn^{II} ion ($S = {}^5/_2$, $g = 2$, $C = 4.375$ cm^3 K mol^{-1}) and two Mn^{III} ions ($S = 2$, $g = 2$, $C = 3$ cm^3 K mol^{-1}) suggesting strong antiferromagnetic interactions in the trinuclear complex. This hypothesis is confirmed by the temperature dependence of the χT product that continuously decreases on lowering the temperature and reaches 1.2 cm^3 K mol^{-1} at 1.8 K. This 1.8 K value is slightly lower than the theoretical value (1.875 cm^3 K mol^{-1}) for the $S_T = {}^3/_2$ ground state expected from the antiferromagnetic coupling of the two Mn^{III} $S = 2$ spins with the Mn^{II} $S = 5/2$ magnetic center. These results suggest that at low temperature the trinuclear complexes of **2** are also antiferromagnetically coupled through weak intermolecular interactions. The field-dependence of the magnetization at 1.8 K supports this idea, and the magnetization does not saturate reaching only 2.2 μ_B at 7 T, rather than the expected value of 3 μ_B (Supporting Information, Figure S1).

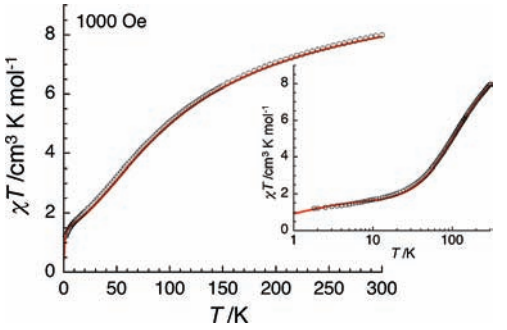

Figure 9. Temperature dependence of the χT product for **2** at 1000 Oe. Inset: Plotting the χT data (open circles) against a logarithmic T scale. The red line is the fit obtained by using a trinuclear model (see text), in which weak intermolecular interactions between the trinuclear units are considered in the frame of the mean field approximation (see text).

(17) Pohl, I. A. M.; Westin, L. G.; Kritikos, M. *Chem. Eur. J.* **2001**, *7*, 3439–3445.

(18) Low, D. M.; Jones, L. F.; Bell, A.; Brechin, E. K.; Mallah, T.; Rivière, E.; Teat, S. J.; McInnes, E. J. L. *Angew. Chem., Int. Ed.* **2003**, *42*, 3781.

To model the temperature dependence of the magnetic susceptibility, we first used a simple symmetrical trinuclear model that assumes the Mn(II)−Mn(III) interactions (J_1) are the same. This is indeed justified by the fact that the central divalent manganese ion resides on an inversion center in the crystal structure (vide supra). In keeping with this structural motif, the isotropic Heisenberg spin Hamiltonian can be written as follows:

$$H = -2J_1(S_{\mathrm{Mn^{III}A}}S_{\mathrm{Mn^{II}}} + S_{\mathrm{Mn^{III}B}}S_{\mathrm{Mn^{II}}})$$

where J_1 is the exchange interaction between adjacent Mn(II) and Mn(III) ions and S_i is the spin operator for each metal center, i (with $S_{\mathrm{MnIII}} = 2$ and $S_{\mathrm{MnII}} = 5/2$). The application of the van Vleck equation[19] to Kambe's vector coupling scheme[20] allows a determination of the low-field analytical expression of the magnetic susceptibility.[21] Although a good agreement between the fit and experimental data was obtained above 14 K, this model was not able to reproduce satisfactorily the susceptibility below 10 K where weak antiferromagnetic inter-trimer interactions (zJ') or magnetic anisotropy (i.e., zero-field splitting) may be relevant. When intermolecular interactions using a mean field approximation are also incorporated into the model,[22] the experimental data can be reproduced very well from 300 to 1.8 K. The best set of parameters found is $J_1/k_B = -9.5(1)$ K, $g = 1.95(2)$, and $zJ'/k_B = -0.37(5)$ K. The magnitude of the interactions between Mn^{II} and Mn^{III} fall in the range of those reported for complexes with an analogous bridging mode (e.g., −10.6 K[21] and −9.7 K for bent Mn^{II}−Mn^{III} and −10.3 K for a linear case[23]). It is should be noted that the estimation of the intermolecular interactions (−0.37 K) is certainly an upper limit as this parameter also contains phenomenologically the magnetic anisotropy of the system. The ac susceptibility measurements performed on **2** and **3** did not show any out-of-phase components, that is compatible with a Single-Molecule Magnet behavior.

The magnetic measurements on **3** were initially performed on a few samples directly after filtration. However, solvent loss means that it is difficult to be precise about the molecular mass of the sample being measured. Therefore, magnetic measurements on compound **3** were also performed directly in a sample in mother liquor. The χT product at room temperature is 63.4 cm^3 K mol^{-1} (Figure 10). This value is in good agreement with the expected value (61.25 cm^3 K mol^{-1}) for the presence of fourteen non-interacting Mn(II) metal ions ($S = {}^5/_2$, $g = 2$, $C = 4.375$ cm^3 K mol^{-1}). On decreasing the temperature, the χT product at 1000 Oe continuously decreases to reach 19.8 cm^3 K mol^{-1} at 1.8 K, suggesting the presence of dominant antiferromagnetic interactions. The field dependence of the magnetization of **3** at 2 K steadily

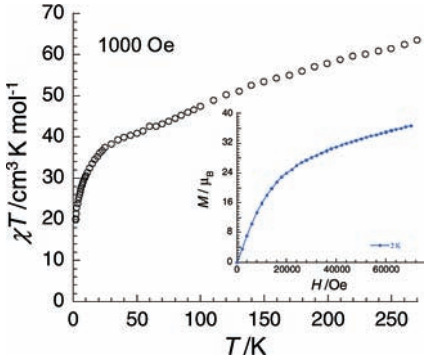

Figure 10. Temperature dependence of the χT product at 1000 Oe for sample of **3** maintained in mother liquor. Inset: Field-dependent magnetization at 2 K. The solid lines are only to guide for the eye.

increases with an increasing dc field until 7 T where it reaches a magnitude of 36.7 μ_B (Figure 10, inset). To get an idea of the spin ground state of this complex, the magnitudes of the χT product at 1.8 K and the high-field magnetization at 2 K can be discussed simultaneously. For the hypothesis that all the spins constituting the $[Mn_{14}]$ complex are strongly coupled in comparison to the thermal energy, the χT value at 1.8 K (19.8 cm^3 K mol^{-1}) suggests a spin ground state that cannot be higher than 6 while the high-field magnetization value indicates the presence of more than 36 spins (inset Figure 10 and Supporting Information, Figure S2). This result demonstrates that the $S = 5/2$ spins in the $[Mn_{14}]$ complex can be aligned easily by the applied magnetic field, in other words that the Mn−Mn intramolecular antiferromagnetic interactions are indeed too weak to stabilize a well-defined ground state at 1.8 K. Unfortunately, it is not possible to deduce the ground state from a detailed analysis of the magnetic interactions within the aggregate as there are more than three distinct magnetic pathways between the Mn^{II} centers, meaning that a simulation of the magnetic susceptibility becomes heavily overparameterized. Therefore, we must conclude that it is not possible to determine the spin ground state of **3** from our magnetic measurements. We also note that the magnetic behavior of **3** is very different from that observed for the tetradecanuclear iron(III) cluster $[Fe_{14}(bta)_6O_6(OMe)_{18}Cl_6]$[18] which was assigned an $S = 23$ spin ground state. This is likely to be the consequence of the different core topology and possibly also the weaker intramolecular magnetic interactions for the differently charged $S = 5/2$ ions (Mn^{2+} versus Fe^{3+}).

Conclusion and Outlook

Using one pot reactions, the manganese compounds **1**, **2**, and **3**, which contain new aryl hydrazone ligands, were produced from the easily synthesized 2-(*N'*-dicyanomethylene-hydrazino)-benzoic acid. The preparations of these compounds illustrate how in situ ligand formations can be useful in the synthesis of new coordination compounds and cluster aggregates. Depending on the location of the ligating sites in the subsequent ligands, chelating and/or bridging species can be formed. Consquently, compounds of varying nuclearities can be obtained. As was observed in compounds **2** and **3**, hydrogen atoms of the resulting ligands may participate in intra- or intermolecular interactions that are

(19) Vleck, J. H. V. *The Theory of Electric and Magnetic Susceptibility*; Oxford University Press: Oxford, U.K., **1932**, .
(20) Kambe, K. *J. Phys. Soc. Jpn.* **1950**, *5*, 48.
(21) Vincent, J. B.; Chang, H. R.; Folting, K.; Huffman, J. C.; Christou, G.; Hendrickson, D. N. *J. Am. Chem. Soc.* **1987**, *19*, 5703–5711.
(22) Li, Y.-G.; Lecren, L.; Wernsdorfer, W.; Clérac, R. *Inorg. Chem. Commun.* **2004**, *7*, 1281–1284.
(23) Kessissoglou, D. P.; Kirk, M. L.; Lah, M. S.; Li, X.; Raptopoulou, C.; Hatfield, W. E.; Pecoraro, V. L. *Inorg. Chem.* **1992**, *31*, 5424–5432.

useful in stabilizing the structure. It is noteworthy that a conventional organic synthetic route to the ligands produced through these in situ reactions is hard to design. On the other hand, there is little prospect of separating the formed ligands from their stabilizing metal centers. Thus, the synthetic methodology can be thought of in terms of a synergistic reaction pathway with all reaction components tending toward a thermodynamically satisfactory product. Evidently, such a synthetic methodology can be useful in targeting new coordination compounds and should be further explored. The examples presented here are molecular whereas previously this technique has been used to produce extended networks.[4] When paramagnetic metals are used in these reactions, they may result in species exhibiting interesting magnetic or electronic properties.

Supporting Information Available: Crystallographic data in CIF file format and further details as noted in the text. This material is available free of charge via the Internet at http://pubs.acs.org.